Science of the Total Environment 644 (2018) 1277–1285

Contents lists available at ScienceDirect

Science of the Total Environment

journal homepage: www.elsevier.com/locate/scitotenv

Removal of antimonate (Sb(V)) and antimonite (Sb(III)) from aqueous solutions by coagulation-flocculation-sedimentation (CFS): Dependence on influencing factors and insights into removal mechanisms

Wenjing Guo [a,b], Zhiyou Fu [b,*], Hao Wang [a,b], Shasha Liu [b], Fengchang Wu [b], John P. Giesy [b,c]

[a] College of Water Sciences, Beijing Normal University, Beijing 100875, China
[b] State Key Laboratory of Environment Criteria and Risk Assessment, Chinese Research Academy of Environmental Sciences, Beijing 100012, China
[c] Department of Biomedical and Veterinary Biosciences, Toxicology Centre, University of Saskatchewan, Saskatoon, Saskatchewan, Canada

HIGHLIGHTS

- Optimum conditions of PFS for the Sb removal were obtained.
- Sb(III) removal has higher priority than that of Sb(V) by CFS.
- The observed experimental results can be explained by the established mechanisms.

GRAPHICAL ABSTRACT

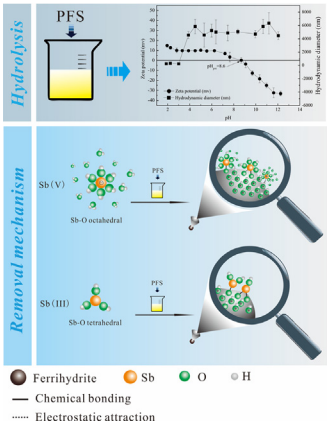

ARTICLE INFO

Article history:
Received 7 May 2018
Received in revised form 30 June 2018
Accepted 3 July 2018
Available online xxxx

Editor: Jay Gan

Keywords:
Polymeric ferric sulfate
Coprecipitation
Characterization
Iron oxyhydroxide
Inorganic antimony species

ABSTRACT

This study investigates the effects of different influence factors on the removal of inorganic Sb species using coagulation-flocculation-sedimentation (CFS) and establishes the mechanism of the process. Thus, the influence of pH, initial Sb concentrations, coagulant dosages and competitive matters on Sb(V) and Sb(III) removal via CFS with polymeric ferric sulfate (PFS) was investigated systemically. Competition experiments and characterization methods, including X-ray diffraction (XRD), energy dispersive spectrometry (EDS), and X-ray photoelectron spectroscopy (XPS), were performed to determine the mechanisms of the process. The main conclusions included: (i) Optimum Sb removal was observed at a pH range of 4–6 and dosages of 4×10^{-4} mol/L and 8×10^{-5} mol/L for Sb(V) and Sb(III), respectively. Additionally, both Sb(V) and Sb(III) removal could be inhibited by the presence of phosphate and humic acid (HA). (ii) A higher priority was observed for the removal of Sb(III) over Sb(V). (iii) After excluding precipitation/inclusion/occlusion, coprecipitation involving chemical bonding played a significant role in both Sb(V) and Sb(III) removal, and electrostatic force served another significant role in Sb(V) removal. The Sb(V) and Sb(III) contamination in real contaminated waters was successfully removed using PFS via CFS process. The results of this study provide insights into the removal mechanisms of inorganic Sb species via CFS.

* Corresponding author.
E-mail address: fuzy@craes.org.cn (Z. Fu).

https://doi.org/10.1016/j.scitotenv.2018.07.034
0048-9697/

1. Introduction

Antimony (Sb) and its compounds are of increasing concern due to their wide application in modern industries and elevated contents in several environmental matrices (Amarasiriwardena and Wu, 2011; Filella et al., 2002a, b; Filella et al., 2007; Filella et al., 2009; He et al., 2012; Herath et al., 2017; Okkenhaug et al., 2011; Wu et al., 2011; Guo et al., 2016). Elevated Sb concentrations have been found in mining areas (Filella et al., 2002a), shooting ranges (Johnson et al., 2005; Steely et al., 2007), and atmospheric particles (Furuta et al., 2005). Particularly in China, the largest Sb producer (Fu et al., 2016; He et al., 2012), elevated Sb concentrations have been detected in surface water contaminated with mine wastewater and residues (Fu et al., 2010; Liu et al., 2010; Wang et al., 2011; Zhu et al., 2009). In recent years, Sb has been gaining negative attention due to its toxic potency and suspected carcinogenicity (Poon et al., 1998; Schnorr et al., 1995). Sb inhalation can damage the respiratory system, liver, and skin of an organism (Gebel et al., 1997). Therefore, Sb and its compounds have been listed as priority pollutants by both the European Union (EU) and the Environmental Protection Agency of the United States (USEPA) (EU, 1976; USEPA, 1979). The maximum admissible Sb concentrations in surface waters in China (5 μg/L, SAC, 2002) and safe drinking water levels established by the World Health Organization (20 μg/L, WHO, 2004) were set to reduce the threat of Sb to human health. Therefore, studies on the removal technology and mechanisms of the two most common Sb species, Sb (V) and Sb(III), in water are crucial.

The main reported pathways for Sb removal from water include coagulation (Du et al., 2014; Guo et al., 2009; Kang et al., 2003; Wu et al., 2010), adsorption (Grafe et al., 2001; Luo et al., 2015; Shan et al., 2014; Wu et al., 2012; Xi et al., 2013; Zhao et al., 2014; Zou et al., 2016), reverse osmosis (Kang et al., 2000), and electrocoagulation (Zhu et al., 2011). Due to its relatively low cost and high efficiency compared to the other removal methods, coagulation, especially by ferric salt, has been frequently applied to purify plants from several heavy metal and NOM (Edwards, 1994; Hering et al., 1997; Kang et al., 2003; Chiang et al., 2009). Polymeric ferric sulfate (PFS), a highly efficient inorganic polymeric ferric flocculant, has been applied in field experiments to remove As from groundwater due to its superior effect, compared to ferric (III) sulfate (Cui et al., 2015). Also, PFS has been used for remediation of accidental contaminants spills in surface waters. For instance, this flocculant was applied during the Sb contamination incident in the Gansu Province in 2015. The contamination was dealt with successfully and the surface water was purified for the residents downstream (Zhang, 2016). Therefore, PFS was selected as the ideal flocculant to study Sb (V) and Sb(III) removal conditions.

Several studies have focused on Sb removal by coagulation and several mechanisms have been suggested: (i) Sb(V) and Sb(III) removal was achieved by coprecipitation, probably via ionic and hydrophobic bonding (Kang et al., 2003); (ii) adsorption mechanism was used to explain Sb removal by coagulation-flocculation-sedimentation (CFS) (Guo et al., 2009); and (iii) surface and internal adsorption, and anomalous incorporation play substantial roles in Sb(V) and Sb(III) removal by ferric salt coagulation (Wu et al., 2010). However, these mechanisms cannot satisfactorily interpret several issues observed in previous studies. For instance, poor Sb(V)/Sb(III) removal at low pH could not be explained by the adsorption mechanism (Guo et al., 2009). Moreover, Sb (III) removal performances were not significantly influenced in the presence of coexisting anions and natural organic matter at higher coagulant dosages (Wu et al., 2010). Additionally, the removal of the homolog of Sb, As(III), was less efficient than that of As(V), while Sb(III) was more efficiently removed by CFS process than Sb(V) (Edwards, 1994; Hering et al., 1997; Guo et al., 2009). Hence, the purification of aqueous solutions by the removal of inorganic Sb species via CFS should be explored to gain further insight into the process.

This study proposes to (i) investigate the influence of pH, initial Sb concentrations, coagulant dosages, and competitive matters on Sb removal via CFS and (ii) explore the removal mechanisms of Sb (V) and Sb(III) by PFS in the CFS process.

2. Materials and methods

2.1. Chemicals and materials

Suwannee River humic acid (HA) was procured from the International Humic Substances Society (IHSS, Colorado, USA). All other chemicals and reagents used in this study were of analytical-reagent grade or greater purity and purchased from Beijing Reagent Co. Stock solutions of Sb(V) and Sb(III) (1000 mg/L) were prepared by dissolving potassium hexahydroxoantimonate ($KSb(OH)_6$; Sigma-Aldrich) and antimony potassium tartrate ($K(SbO)C_4H_4O_6$; Sinopharm Chemical Reagent Co. Ltd.), respectively. Deionized water (18.2 MΩ·cm) was generated using a Milli-Q system.

2.2. Batch coagulation experiment

The coagulant stock solution was prepared by dissolving PFS powder (Fe concentration = 18.5%, basicity = 9.0–14.0%, pH = 2.0–3.0, Tianjin Guangfu Fine Chemical Research Institute) in deionized water. A 97.2 m^2/g BET N_2 surface area (Micromeritics, TriStar II 3020, Norcross, USA) and scanning electron microscope image (SEM; Fig. S1, SU8010, Horiba scientific) of the coagulant were obtained. The alkalinity of natural water was simulated by adding 4.0×10^{-3} mol/L $NaHCO_3$ to deionized water. Synthetic test water samples with various Sb contents were prepared by spiking with stock solutions of Sb(V) and Sb(III).

Jar tests were conducted using a stainless-steel stirrer and six beakers (HJ-6, Jintan Electics Cor. China). Approximately 200 mL of the test water was transferred into a 500-mL beaker. Predetermined amounts of PFS were then dosed into the beakers to produce nominal Fe concentrations. Subsequently, the pH of the test water samples were adjusted to predetermined pH through dropwise addition of 0.15 mol/L HCl and 0.3 mol/L NaOH. The solution was stirred rapidly at a speed of 140 rpm for 3 min, and subsequently at 40 rpm for 20 min. After 30 min of quiescent settling, the supernatant solution of the test water sample was collected and filtered through 0.45-μm nylon membrane filters (Whatman, UK). Finally, the test samples were collected and used for the determination of Sb(V) and Sb(III) concentrations.

pH values ranging from 2 to 12 were tested to determine the optimum pH for Sb(V) and Sb(III) removal by CFS. Since the removal capacity of the coagulants was higher for Sb(III) than for Sb(V), relatively low PFS contents (1/20–1/5 of the amount of the coagulants used for Sb(V)) were used when investigating the removal of Sb(III) (Guo et al., 2009; Kang et al., 2003; Ungureanu et al., 2015). The potential effects of phosphate (0–4 mg P/L as P) and HA (0–4 mg C/L) on Sb removal by PFS in the CFS process, at the optimum pH, were then assessed.

Under light illumination, Sb(III) could be oxidized to Sb(V) in the presence of inorganic Fe(III) (Kong et al., 2016). Oxidization of Sb(III), at low concentrations, was also observed in our pre-experiments. Therefore, all the tubes and beakers were capped and wrapped with aluminum foil to exclude light. Experiments to determine the effects of competition on Sb(V) and Sb(III) (250 and 100 μg/L, respectively) removal were also performed. To investigate the difference in the Sb (V) (500 μg/L) removal performance in the presence of Sb(III) (400 μg/L), concentrations of Sb(V) were measured before and after the addition of the Sb(III) stock solutions with a coagulant dosage of 8×10^{-4} mol/L. The amount of Sb(III) (400 μg/L) removal in the presence and absence of Sb(V) (500 μg/L) was also measured.

2.3. Coagulant characterization

In order to guarantee that the newly formed Sb phase and products of PFS loaded with Sb(V)/Sb(III) in the CFS process for subsequent

determination, relatively large amounts of Sb(V)/Sb(III) (100 mg/L) and PFS (1.6×10^{-3} mol/L as Fe) were added to de-ionized water (200 mL) at the optimum pH. The same concentration of PFS was added to water to obtain pure PFS products. Solid products were collected by centrifugation, and then the precipitate was washed at least three times with de-ionized water and frozen dried at −24 °C for at least 3 days.

The pure PFS and its products in Sb(V)/Sb(III) removal were analyzed by an SEM equipped with EDS. Prior to imaging, the sample was sputtered with gold in a vacuum condition for 30 s. X-ray diffraction (XRD) patterns of flocculation were obtained by using XRD analysis (D8 advance, Bruker, Germany). Elemental compositions of the samples were determined via X-ray photoelectron spectroscopy (XPS; PHI Quantera SXM, ULVAC-PHI, Japan), with a monochromated X-ray beam (100 μm) from an Al target at an angle of 45°. The binding energy was calibrated with C1s of 284.8 eV.

2.4. Analytical methods

High performance liquid chromatography-hydride generation-atomic fluorescence spectrometry (HPLC-HG-AFS, Millennium Excalibur System, Kent, United Kingdom) was used to determine the inorganic Sb species. An anion exchange column (PRP-X100, 4.1 × 250 mm, 10 μm) was used to separate Sb(V) and Sb(III). The conditions for the HPLC-HG-AFS were as follows: ammonium tartrate solution (pH value was adjusted to 5; purchased from Sinopharm Chemical Reagent Co., Ltd) was used as a mobile phase with a flow rate of 1.0 mL/min. The carrier solutions of 1.8 mol/L HCl and 0.8% $NaBH_4$ solution (mass ratio) for HG-AFS was prepared with ultrapure hydrochloric acid and powdered $NaBH_4$ (both purchased from Tianjin Fuchen Chemical Reagents Factory) in 0.4% NaOH solution (mass ratio), respectively. The sample injection volume was 200 μL and the Sb species were determined by PSA-10.055 (P S Analytical). Seven mixed standard solutions of Sb(V) and Sb(III) (0 to 100 μg/L) were obtained by mixing stock solutions, which were prepared by diluting stock solutions of $KSb(OH)_6$ and $K(SbO)C_4H_4O_6$. The operating conditions of the AFS instrument were optimized and the calibration curves of Sb(V) and Sb(III) exhibited good linearity (both correlation coefficients exceeded 0.999). The concentrations of Sb species were obtained by the calculated peak area using the SAMCal software.

The limits of detection (LOD) of Sb(V) and Sb(III) were 0.015 and 0.55 μg/L, respectively with relative standard deviations (RSDs) of the duplicated samples of <5%. The pH values of the test water samples were measured with a pH meter (FE20K, Mettler Toledo, Switzerland). The ζ potential and hydrodynamic diameter (HDD) of flocculation in the aqueous solutions were measured with a Zetasizer nanometer (Malvern, England).

3. Results and discussion

3.1. Effects of pH, contaminant, coagulation dosage and competitive matters on Sb removal

3.1.1. Effects of pH on Sb removal by coagulation

Removal of Sb(V) and Sb(III) by CFS with PFS varied as a function of pH (Fig. 1). For Sb(V) (250 μg/L), removal efficiencies of 60.3% (pH = 2.9) and 73.5% (pH = 2.5) were observed at respective PFS concentrations of 8×10^{-4} mol/L and 4×10^{-4} mol/L as Fe. On the other hand, when the pH was increased to 3.9 and 3.1, Sb(V) removal increased sharply to ~99.7% (8×10^{-4} mol/L PFS as Fe) and 94.8% (4×10^{-4} mol/L PFS as Fe). At a pH range of 6–11, Sb(V) elimination decreased slowly with an increase in pH. With a further increase in pH (pH = 10–11), 30–40% Sb(V) removal was observed for both PFS concentrations. A pH of 5 was selected as the optimum pH for the subsequent batch experiments.

The effects of pH on Sb(V) removal were consistent with results of previous study (Guo et al., 2009). The hydrolyzation of ferric salts was demonstrated in Eqs. (1)–(3) (Duan and Gregory, 2003; Matijević and Scheiner, 1978):

$$Fe(H_2O)_6^{3+} + nH_2O \leftrightharpoons \left[Fe(OH)_n(H_2O)_{6-n}\right]^{(3-n)+} + nH_3O^+ \quad (1)$$

$$\left[Fe(OH)^{2+}\right]_n + Fe^{3+} + 2H_2O \leftrightharpoons \left[Fe(OH)^{2+}\right]_{n+1} + 2H^+ \quad (2)$$

$$\left[Fe(OH)^{2+}\right]_n \leftrightharpoons [FeO(OH)]_n + nH^+ \quad (3)$$

The hydrolyzation of PFS is more complex than that of monomeric ferric salts, as iron ions in PFS have hydrolyzed and polymerized, and these polymeric salts have aged prior to use. Various iron oxyhydroxides complexes, including monomers, dimers, medium molecular weight polymers and high molecular weight polymers, form afterwards in the aqueous solution (Jiang and Graham, 1998; Jiang et al., 1993; Cheng, 2002). These complexes can carry more positive charges and have greater specific surface areas in aqueous solution. The equilibria of the ferric salts shift to the left with decrease in pH. The results from this study supported this hydrolyzation mechanism. At pH values <4, the hydrodynamic diameter of the polynuclear polymer decreased (Fig. 2), and ionization of the PFS hydrolysate resulted in a poorer removal capacity. This mechanism is probably responsible for the poor Sb(V) removal by PFS at lower pH values in both a previous study (Guo et al., 2009) and in this study (Fig. 1a and b).

Poor Sb(III) (100 μg/L) removal of 10–20% was observed at pH values <3 (Fig. 1c and d). Sb(III) removal increased gradually with an increase in pH and reached consistent removal rates (>90%) at pH values >5.4 (4×10^{-5} mol/L) and > 8.1 (2×10^{-5} mol/L). The superior Sb(III) removal rates at higher pH observed in this study was attributed to the fate that: the main form of Sb(III) in natural water, $Sb(OH)_3$, is electrically neutral. Thus, with increasing hydrodynamic diameter and loosening of the structure, Sb(III) is mostly removed via sweep coagulation by the PFS hydrolysate (Fig. 2).

3.1.2. Effects of the initial coagulant and Sb concentrations on Sb removal

The percentage of Sb(V) removal was greatly influenced by the initial PFS and Sb concentrations (Fig. 3a). Sb(V) removal reached 88.1% when the PFS concentration was 2×10^{-4} mol/L as Fe and the initial concentration of Sb(V) was 250 μg/L. Moreover, the proportion of removed Sb(V) increased gradually as a function of increasing PFS concentration. At an initial PFS concentration of >8×10^{-4} mol/L, Sb (V) removal reached a plateau of 99–100%. The proportion of Sb (V) removal decreased gradually, depending on the initial Sb (V) concentrations (250–1000 μg/L). Similarly, the initial PFS and Sb concentrations affected Sb(III) removal (Fig. 3b). The optimum removal efficiency was achieved at coagulant dosages of 4×10^{-4} mol/L for Sb (V) and 8×10^{-5} mol/L for Sb(III). Notably, these results confirmed that the removal efficiency of Sb(III) was greater than that of Sb(V).

3.1.3. Effects of phosphate and HA on Sb(V) and Sb(III) removal

The addition of PO_4^{3-} ions at different PFS concentrations significantly inhibited Sb(V) removal (250 μg/L, Fig. 4a). For example, when the concentration of PFS was 6×10^{-4} mol/L, 96.7, 94.0, and 88.6% Sb (V) removal was achieved at PO_4^{3-} concentrations of 0, 1, and 2 mg P/L, respectively. The PO_4^{3-} ions also interfered with Sb(III) removal (100 μg/L, Fig. 4b). The results of this study were not consistent with the conclusions on Sb removal by ferric salts reported in the literature (Wu et al., 2010). This study suggested that compared to Sb (V) removal, Sb(III) removal was not significantly inhibited PO_4^{3-} at higher ferric salt dosage. This difference might be attributed to the excess coagulant employed for higher ferric chloride dosages so that the interfering ions had little effect on Sb(III) removal. The lower removal in the presence of PO_4^{3-} is attributed to the fact that P and Sb are group V elements with the same s2p3 configuration in their outermost

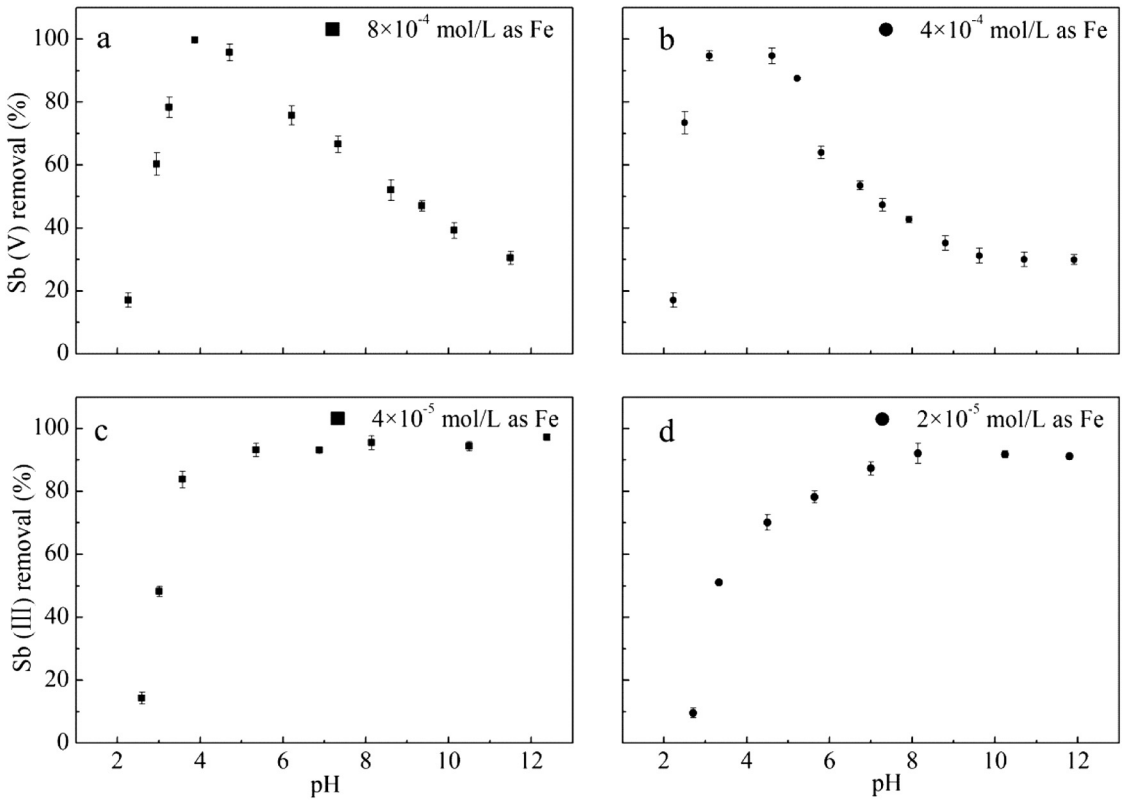

Fig. 1. Effect of pH on Sb removal from aqueous solutions: (a) Sb(V) with 8×10^{-4} mol/L polymeric ferric sulfate (PFS); (b) Sb(V) with 4×10^{-4} mol/L PFS; (c) Sb(III) with 4×10^{-5} mol/L PFS, and (d) Sb(III) with 2×10^{-5} mol/L mM PFS. Temperature: 25 ± 1 °C, initial Sb(V) and Sb(III) concentrations: 250 and 100 μg/L, respectively.

shell. Thus, their similar chemical properties resulted in strong competition for sorption sites between the PO_4^{3-} and Sb species (Okkenhaug et al., 2012).

HA also interfered with and decreased Sb(V) (250 μg/L) removal (Fig. 4c). For example, at a PFS concentration of 6×10^{-4} mol/L, Sb (V) removal decreased from 96.7%, in the absence of HA, to 94.1%, in the presence of 2 mg C/L, and 90.6%, in the presence of 4 mg C/L. Sb (III) (100 μg/L) removal by PFS was also inhibited by HA, especially at low PFS concentrations (Fig. 4d). The conclusion that Sb(V) and Sb(III) removal was inhibited by HA, was not consistent with results from previous studies which reported that Sb(III) removal was not inhibited by HA at higher coagulant dose (Wu et al., 2010). The reason for the difference in the effects of both HA and PO_4^{3-} on Sb(III) removal were similar in that, in the presence of sufficient coagulant the effects of these two chemicals were minimal at higher ferric chloride dosages. The lower Sb(V) and Sb(III) removal in the presence of HA occurs because HA can bind with Sb and remove it from the solution phase (Steely et al., 2007). Therefore, HA competes for several of the available reactive sites for Sb(V) or Sb(III) removal by several binding sites (i.e. surface complexation). During Sb(III) removal, HA has the ability to oxidize from Sb(III) to Sb(V), possibly in the presence of quinone and/or

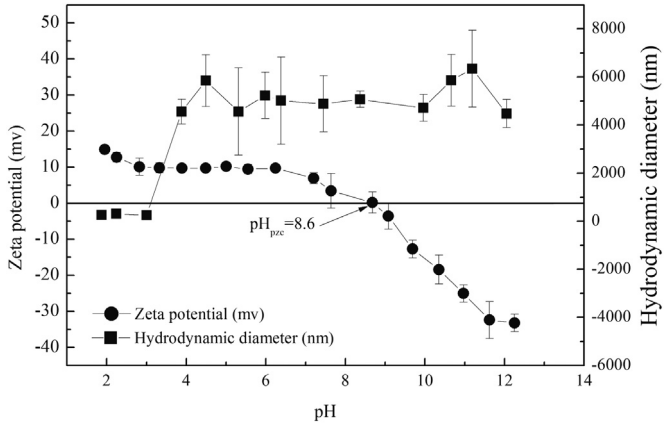

Fig. 2. Effect of pH on the ζ potential and hydrodynamic diameter of polymeric ferric sulfate (PFS) in aqueous solution; initial concentration of PFS dosage: 8×10^{-4} mol/L as Fe.

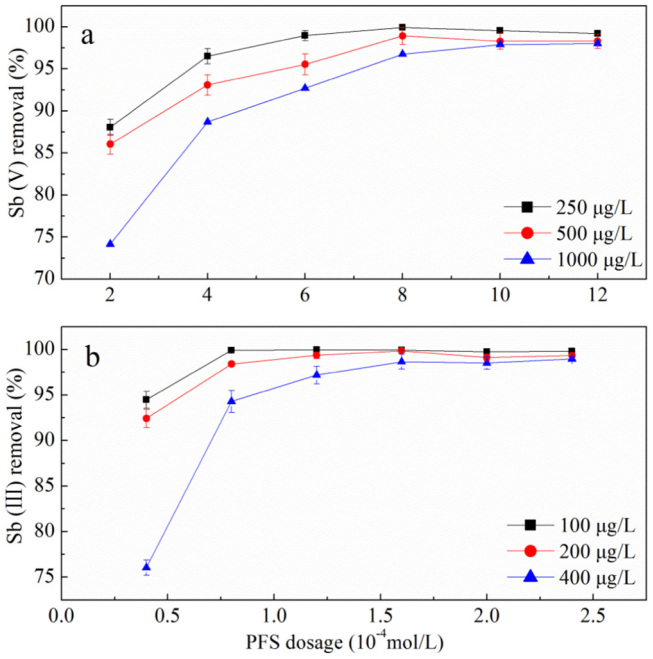

Fig. 3. Removal of (a) Sb(V) and (b) Sb(III) by coagulation as a function of polymeric ferric sulfate (PFS) concentration at different Sb concentrations. Temperature: 25 ± 1 °C and pH: 5.0 ± 1.0.

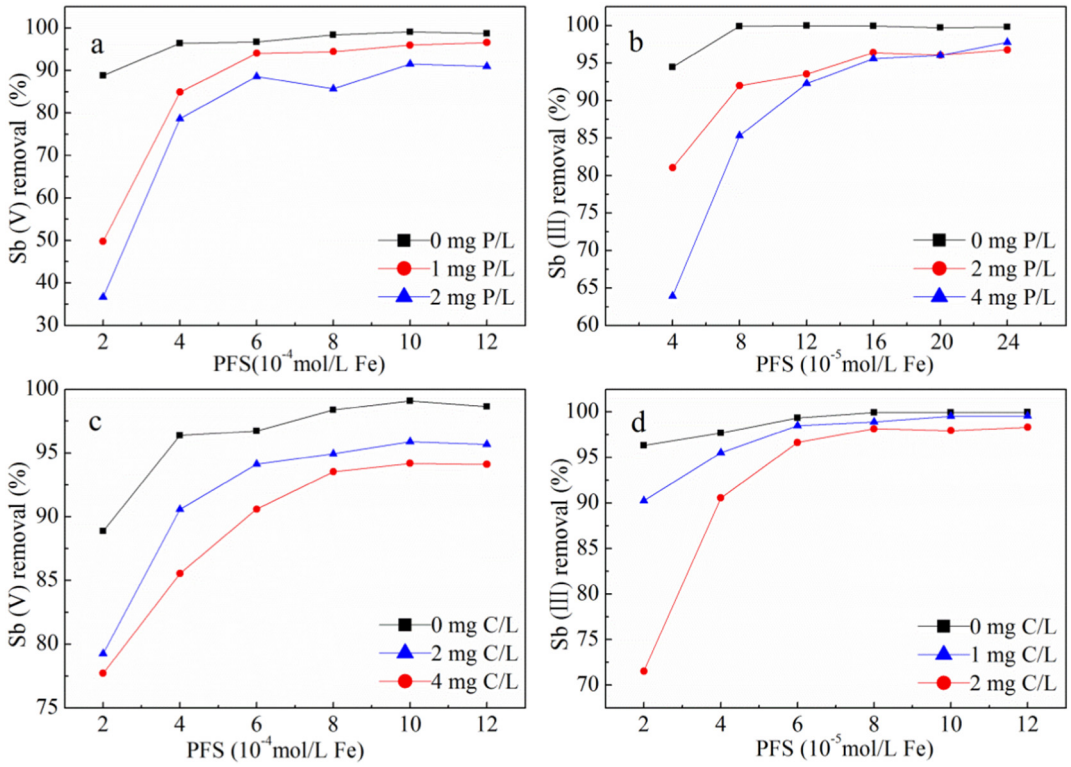

Fig. 4. Effect of phosphate on (a) Sb(V) and (b) Sb(III) removal via CFS process with polymeric ferric sulfate (PFS). The effect of humic acid (HA) on (c) Sb(V) and (d) Sb(III) removal via CFS process by PFS. Temperature: 25 ± 1 °C, initial Sb(V) and Sb(III) concentrations: 250 and 100 μg/L, respectively; pH: 5.0 ± 0.1.

disulfide functional groups (Buschmann and Sigg, 2004; Buschmann et al., 2005; Dorjee et al., 2014; Steely et al., 2007; Ceriotti and Amarasiriwardena, 2009). Hence, Sb removal decreases due to the relatively poor removal efficiency of Sb(V). Overall, not only Sb(V), but Sb (III) removal was also influenced by competitive matters such as phosphate and HA at higher PFS concentrations.

3.2. Competitive removal of the Sb species by CFS

When Sb(V) (250 μg/L) and Sb(III) (100 μg/L) were both present in the aqueous solution, the percentage removal of Sb(III) was greater than that of Sb(V) (Fig. 5A). Sb(III) removal was 98.5% in the presence of 2×10^{-4} mol/L PFS and ranged between 98.5 and 99.7% in the presence of excess PFS coagulant. On the other hand, a relatively lower Sb (V) removal (93.2%) was observed when 2×10^{-4} mol/L PFS was added, while the percentage removal increased at greater PFS concentrations.

The removal percentage of Sb(V) at a concentration of 500 μg/L in the presence of 400 μg Sb(III)/L (68.1 ± 1.8%, n = 3, Fig. 5(b)) was less than that observed in the absence of Sb(III) (85.2 ± 3.4%, n = 3, Fig. 5(a)). On the other hand, the removal percentage of Sb(III) at a concentration of 400 μg/L in the presence of 500 μg Sb(V)/L (96.5 ± 0.9%, n = 3, Fig. 5(d)) was slightly less than that observed in the absence of the competing Sb(V) species (99.1 ± 0.6%, n = 3, Fig. 5(c)). These results suggest that Sb(III) is preferentially removed by PFS in the CFS process.

3.3. Characterization of the pure PFS and its Sb(V) and Sb(III) products

3.3.1. XRD analyses

The XRD patterns recorded when PFS was exposured to Sb(V) and Sb(III) were analogous to that of the pure PFS, whereby all the patterns

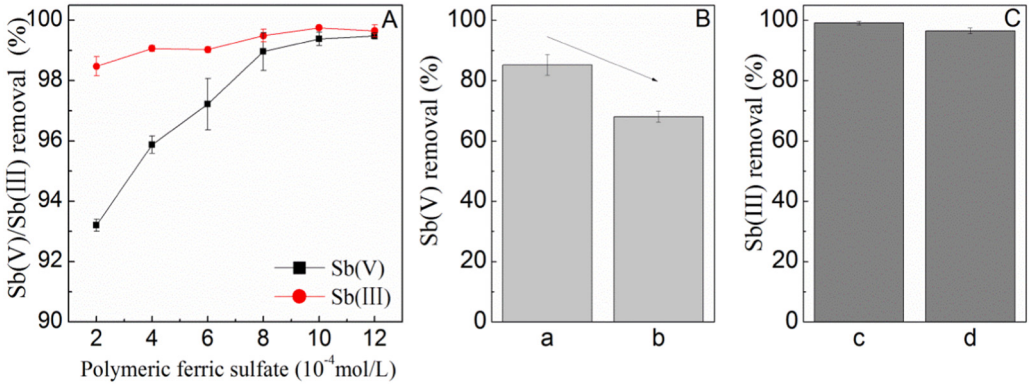

Fig. 5. A: Percentage Sb(V) and Sb(III) when both species were added to the test water samples; initial Sb(V) and Sb(III) concentrations: 250 and 100 μg/L, respectively. B: (a) percentage removal of Sb(V) (concentration: 500 μg/L); (b) percentage removal of Sb(V) (concentration: 500 μg Sb(V)/L in the presence of 400 μg Sb(III)/L). C: (c) percentage Sb(III) removal (concentration: 400 μg/L); (d) percentage Sb(III) removal (concentration: 400 μg Sb(III)/L in the presence of 500 μg Sb(V)/L). Temperature: 25 ± 1 °C, pH: 5.0 ± 0.1.

peaked with broad bands at respective 2θ angles of 34° and 60° (Fig. 6). These similarities indicated that the inner crystal structure of the products produced by the interaction of PFS with Sb(V) and Sb(III) was not altered.

The likely mechanisms of removal by ferric salts, which convert the inorganic Sb species to insoluble products, were precipitation and coprecipitation with iron oxyhydroxide (Edwards, 1994). However, the Sb(V) and Sb(III) residual concentrations were not in the same range as the different initial Sb concentrations due to the formation of $FeSbO_4$ for Sb(V) and $FeSbO_3$ or Sb_2O_3 for Sb(III) in solution. This suggests that the potential Sb(V) and Sb(III) removal mechanisms did not include precipitation. Therefore, coprecipitation, including isomorphic/nonisomorphic inclusion, occlusion, and surface adsorption, is the most likely Sb removal mechanism (Duan and Gregory, 2003; Kurniawan et al., 2006). Since the ionic radius of Sb^{3+} (0.076 nm) is larger than that of Fe^{3+} (0.064 nm), nonisomorphic inclusion would distort the inner crystal structure and alter the XRD patterns. Additionally, the coprecipitation law suggests that inclusion did not occur between the miscible trace element (Sb^{5+}) and the macrocomponent (Fe^{3+}) with non-equal valence. Thus, inclusion of Sb(V)/Sb(III) into iron oxyhydroxide should be disregarded. Occlusion could also result in the distortion of the inner crystal structure and is therefore not likely Sb removal mechanism. Thus, surface adsorption, involving van der Waals forces, electrostatic interactions, and chemical bonding, is the most likely mechanism responsible for Sb removal during the CFS process.

3.3.2. EDS analyses

EDS was used to investigate the elemental contents of PFS and the products formed when PFS was bound to Sb(V) or Sb(III) (Table 1). Different elemental contents were observed for PFS, PFS-Sb(V), and PFS-Sb(III). The proportion of oxygen (O) in PFS-Sb(V) was 48.1%, which was greater than that of PFS (37.8%) and PFS-Sb(III) (30.1%). In addition, Sb/Fe was almost constant in Sb(V) and Sb(III) removal, while the molar atomic ratio of O/Sb(V) was approximately twice that of O/Sb(III). The higher oxygen proportion might indicate different interaction types between Sb(V)/Sb(III) and PFS.

3.3.3. XPS analyses

The Fe 2p XPS spectra in the absence and presence of Sb(V) and Sb(III) did not change (Fig. S2), thereby indicating that the Fe was not involved in Sb removal. High resolution O 1s spectra of the iron oxyhydroxide in the absence and presence of Sb(V) and Sb(III) are presented in Fig. 7a. The spectrum of pure PFS presented peaks at 531.6 eV for O 1s, while products of PFS in the presence of Sb(V) and Sb(III) displayed peaks at two energy positions corresponding to O 1s and Sb $3d_{3/2}$, respectively. Peaks associated with Sb $3d_{3/2}$ at a binding energy of 540.19 eV (iron oxyhydroxide loading with Sb(V)) and 539.77 eV (iron oxyhydroxide loading with Sb(III)) were attributed to the

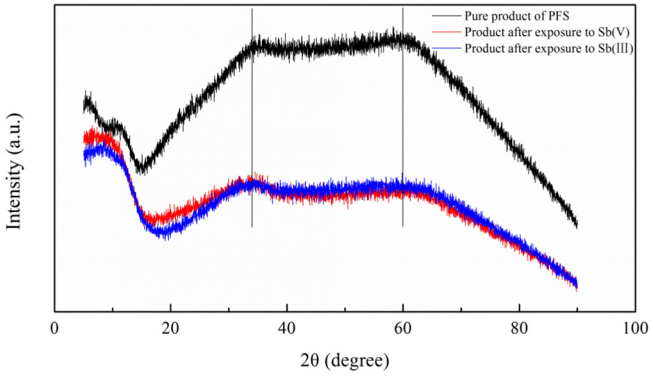

Fig. 6. X-ray diffraction (XRD) patterns of the pure polymeric ferric sulfate (PFS) hydrolysate and combinations of PFS with Sb(V) and Sb(III).

Table 1
Percentage of atomic contents based on energy dispersive spectrometry (EDS) analyses.

Sample types	Percentage of atomic content (%)				Sb/Fe	O/Sb
	Fe	O	S	Sb		
Pure polymeric ferric sulfate (PFS)	57.9 ± 0.4	37.8 ± 0.4	4.3 ± 0.2	0	/	/
PFS after exposure to Sb(V)	43.2 ± 0.3	48.1 ± 0.3	4.6 ± 0.1	4.2 ± 0.2	0.097	11.45
PFS after exposure to Sb (III)	59.4 ± 0.4	30.1 ± 0.3	5.1 ± 0.2	5.4 ± 0.1	0.091	5.57

combination of the existing Sb with the products. Compared to the O 1s binding energy (531.7 eV) in pure iron oxyhydroxide, the O 1s binding energy of the iron oxyhydroxide adsorbed with Sb(V) and Sb(III) decreased to 530.8 and 530.6 eV, respectively. This lower binding energy can be attributed to the chemical reactions of Sb and O on the surface of the iron oxyhydroxide. Overall, the O1s XPS spectra suggested that both Sb(V) and Sb(III) underwent chemical reactions with the iron oxyhydroxide.

The peaks associated with the O 1s and Sb 3d were deconvoluted into three or four peaks (Fig. 7b). The value of the O_{ad}/Sb $3d_{5/2}$ ratio, which is the ratio of adsorbed oxygen to Sb $3d_{5/2}$, decreased from 0.77

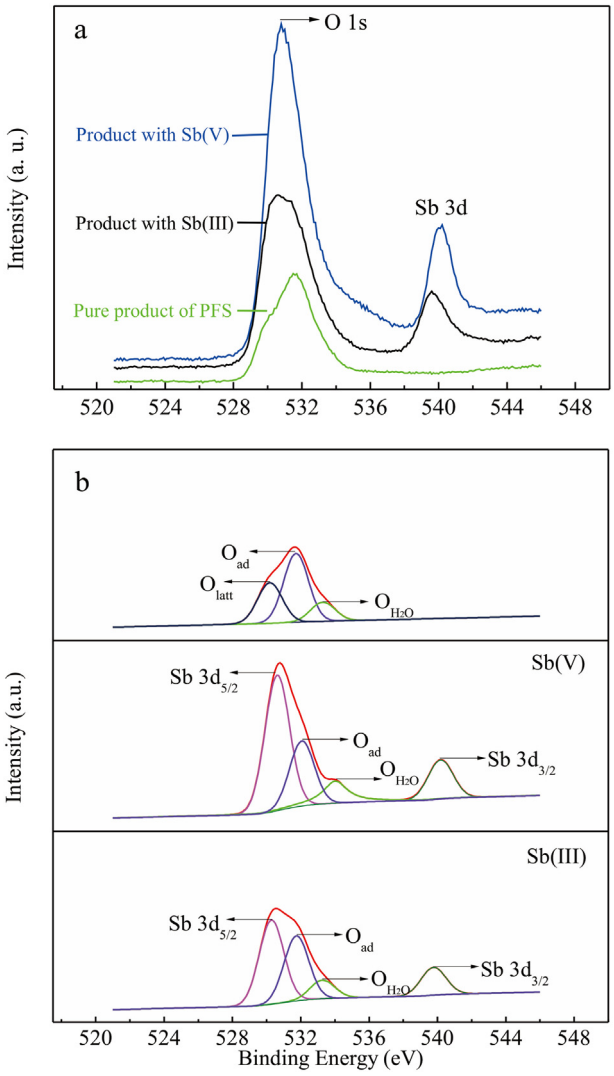

Fig. 7. (a) X-ray photoelectron spectroscopy (XPS) spectra of the iron oxyhydroxide in the absence and presence of Sb(V) and Sb(III); (b) deconvoluted results of the O 1 s and Sb 3d levels of the XPS spectra.

(Sb(III)) to 0.48 when Sb(V) was adsorbed by iron oxyhydroxide (Table S1). It was postulated that both Sb(V) and Sb(III) were chemically bonded to the iron oxyhydroxide; since Sb(V) and Sb(III) are associated with six and three —OH groups, respectively, the same Sb(V) and Sb(III) removal mechanism could result in a higher O_{ad}-to-Sb $3d_{5/2}$ ratio during Sb(V) removal (Luo et al., 2015). Thus, the lower O_{ad}-to-Sb $3d_{5/2}$ ratio observed during Sb(V) removal suggested that there might be other interactions, apart from chemical bonding, involved in Sb removal.

3.4. Sb(V) and Sb(III) removal mechanisms in the CFS process

Previous studies have suggested that Sb(V) and Sb(III) removal in the CFS process occurs via adsorption, internal adsorption, ionic bonding, or hydrophobic bonding (Guo et al., 2009; Kang et al., 2003; Wu et al., 2010). However, these mechanisms cannot provide a satisfactory explanation for several experimental results observed in this study. These include, the greater independence of Sb(III) removal over that of Sb(V) in the presence of competitive matters; the variation in removal performance as a function of pH; the unaltered XRD patterns observed in this study; and the higher priority of Sb(III) removal compared to Sb(V) removal via the CFS process.

XPS analyses revealed that Sb(V) and Sb(III) underwent chemical reactions with the PFS products. Thus, chemical bonding was established as the dominant interaction between Sb and the iron oxyhydroxide. Similar to As, the most plausible chemical interactions between Sb and the PFS products were the formation of inner sphere complexes with —OH functional groups at the surface of the iron oxyhydroxide (Guo et al., 2014; Mitsunobu et al., 2013; Mitsunobu et al., 2010; Shan et al., 2014; Xi et al., 2013) (Fig. 8). While for Sb(V), considering that the Sb (V) removal performance decreased at pH >6, another likely interaction between Sb(V) (common form: $Sb(OH)_6^-$) and the PFS products (their charge was presented in Fig. 2) could be electrostatic attraction. Hence, electrostatic forces also played a significant role in Sb (V) removal via CFS process (Fig. 8).

The bonding energy of the electrostatic attractions was less than that of the chemical reactions. Thus, coprecipitation between Sb(V) and the iron oxyhydroxide was weaker than that of Sb(III) because the binding of Sb(V) to the iron oxyhydroxide was partly due to electrostatic attraction. These Sb(V) and Sb(III) coprecipitation mechanisms could explain the following phenomena: i) Sb(III) removal exhibited greater independence from CFS than Sb(V) in the presence of phosphate and HA from this study and previous study (Guo et al., 2009) and ii) the high priority of Sb(III) removal in the competition experiments via CFS process (Section 3.2). Furthermore, Sb(V) associates with six —OH groups to form Sb—O octahedral geometry (Fig. 8), while Sb(III) is bound to only three —OH groups to form Sb—O tetrahedral geometry (Fig. 8). Sb(V) was wrapped by layers of water molecules via Van der Waals

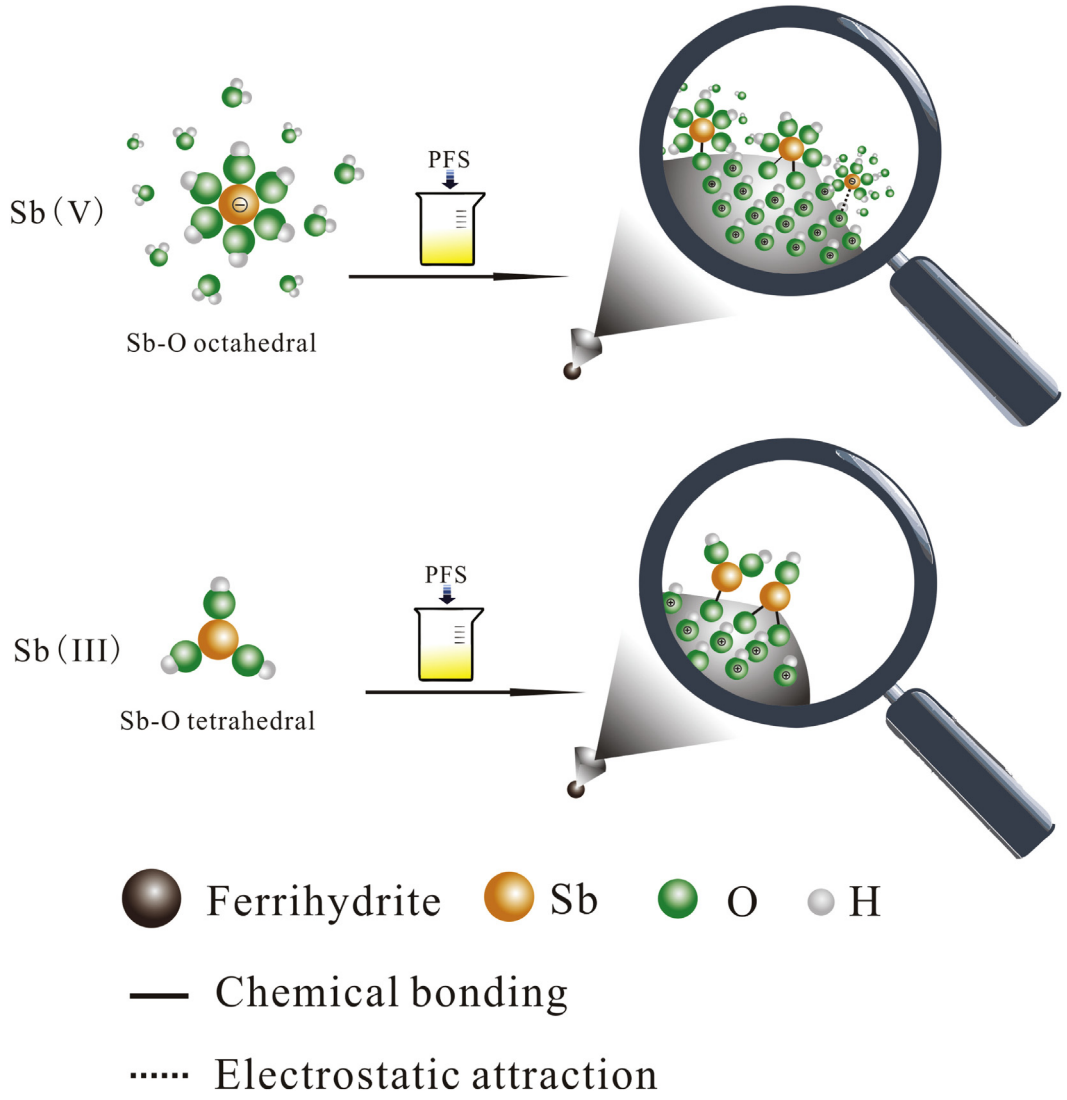

Fig. 8. Possible interactions of (a) Sb(V) and (b) Sb(III) in aqueous solutions with PFS during the coagulation-flocculation-sedimentation (CFS) process; pH: 5.0 ± 1.0.

force in natural water, while Sb(III) formed exposed and neutral molecules without any layers of water molecules. Thus, the larger molecular size of Sb(V), relative to that of Sb(III), could also explain the following results: iii) the removal capacities of Sb(V) by CFS was significantly less than that observed for Sb(III) (Section 3.1.2); and iv) the high elemental composition of oxygen and low O_{ad}/Sb $3d_{5/2}$ ratio in PFS bound to Sb (V) as determined by EDS and XPS analyses, respectively (Sections 3.3.2 and 3.3.3).

3.5. Application in real surface water

The Sb removal performance of CFS process in surface waters was examined by using real contaminated water. The surface water samples were collected from the Xikuangshan mining area in Hunan province, China, which was one of the world's major producers of Sb and nicknamed as the "World's Antimony Capital" (Fu et al., 2016; He et al., 2012). The aquatic parameters of different types of surface waters, including river water, retained water, and well water, are provided in Table S2 of supplementary materials. In order to simulate the high levels of Sb in surface water, samples were spiked with stock solutions of Sb (V) (250 μg/L) and Sb(III) (100 μg/L) respectively.

The Sb removal performances of CFS process that presented in Table S3 showed that treatment with PFS at pH 5.0 ± 0.1 could achieve Sb(V) and Sb(III) removal percentages of >96.0% and >98.1%, respectively. The residual concentrations of Sb(V) and Sb(III) were < 10.0 and <1.9 μg/L, respectively, which was in compliance with the safe drinking water levels of WHO (20 μg/L, WHO, 2004). The simulated experiments indicated that Sb removal using the CFS process is a promising method to treat real water.

4. Conclusions

In this study, optimum Sb removal efficiency was achieved at a pH range of 4–6 at dosages of 4×10^{-4} mol/L for Sb(V) and 8×10^{-5} mol/L for Sb(III). Both Sb(V) and Sb(III) removal were influenced by the initial Sb concentration, coagulant dosage, and presence of phosphate or humic acid. The removal priority by PFS of Sb(III) was higher than that of Sb(V) in aqueous solutions. Coprecipitation, which attributed Sb(V)/Sb(III) removal to chemical reactions and Sb (V) removal to electrostatic attractions, was established as the main removal mechanism in the CFS process. The proposed mechanisms have provided new insights into Sb removal by PFS in the CFS process, and explain the differences between the Sb(V) and Sb(III) removal performances of the CFS process.

Acknowledgements

This research was supported by the National Natural Science Foundation of China (41473109) and China Postdoctoral Science Foundation (2017M622280).

Appendix A. Supplementary data

Tables of S1–S2 and figures of S1–S3 are presented in the supplementary materials. Supplementary data to this article can be found online at https://doi.org/10.1016/j.scitotenv.2018.07.034.

References

Amarasiriwardena, D., Wu, F., 2011. Antimony: emerging toxic contaminant in the environment. Microchem. J. 97, 1–3.
Buschmann, J., Sigg, L., 2004. Antimony (III) binding to humic substances: influence of pH and type of humic acid. Environ. Sci. Technol. 38, 4535–4541.
Buschmann, J., Silvio Canonica, A., Sigg, L., 2005. Photoinduced oxidation of antimony(III) in the presence of humic acid. Environ. Sci. Technol. 39, 5335–5341.
Ceriotti, G., Amarasiriwardena, D., 2009. A study of antimony complexed to soil-derived humic acids and inorganic antimony species along a Massachusetts highway. Microchem. J. 91, 85–93.
Cheng, W.P., 2002. Comparison of hydrolysis/coagulation behavior of polymeric and monomeric iron coagulants in humic acid solution. Chemosphere 47, 963–969.
Chiang, P.C., Chang, E.E., Chang, P.C., Huang, C.P., 2009. Effects of pre-ozonation on the removal of THM precursors by coagulation. Sci. Total Environ. 407, 5735–5742.
Cui, J., Jing, C., Che, D., Zhang, J., Duan, S., 2015. Groundwater arsenic removal by coagulation using ferric (III) sulfate and polyferric sulfate: a comparative and mechanistic study. J. Environ. Sci. 32, 42–53.
Dorjee, P., Amarasiriwardena, D., Xing, B., 2014. Antimony adsorption by zero-valent iron nanoparticles (nZVI): ion chromatography–inductively coupled plasma mass spectrometry (IC–ICP-MS) study. Microchem. J. 116, 15–23.
Du, X., Qu, F., Liang, H., Li, K., Yu, H., Bai, L., Li, G., 2014. Removal of antimony (III) from polluted surface water using a hybrid coagulation–flocculation–ultrafiltration (CF–UF) process. Chem. Eng. J. 254, 293–301.
Duan, J., Gregory, J., 2003. Coagulation by hydrolysing metal salts. Adv. Colloid Interf. Sci. 100, 475–502.
Edwards, M., 1994. Chemistry of arsenic removal during coagulation and Fe–Mn oxidation. J. Am. Water Works Assoc. 86, 64–78.
EU, 1976. Council Directive 76/464/EEC of 4 May 1976 on Pollution Caused by Certain Dangerous Substances Discharged Into the Aquatic Environment of the Community, Off. J. L. 129 pp. 23–29.
Filella, M., Belzile, N., Chen, Y.-W., 2002a. Antimony in the environment: a review focused on natural waters: I. Occurrence. Earth-Sci. Rev. 57, 125–176.
Filella, M., Belzile, N., Chen, Y.-W., 2002b. Antimony in the environment: a review focused on natural waters: II. Relevant solution chemistry. Earth-Sci. Rev. 59, 265–285.
Filella, M., Belzile, N., Lett, M.-C., 2007. Antimony in the environment: a review focused on natural waters. III. Microbiota relevant interactions. Earth-Sci. Rev. 80, 195–217.
Filella, M., Williams, P.A., Belzile, N., 2009. Antimony in the environment: knowns and unknowns. Environ. Chem. 6, 95–105.
Fu, Z., Wu, F., Amarasiriwardena, D., Mo, C., Liu, B., Zhu, J., Deng, Q., Liao, H., 2010. Antimony, arsenic and mercury in the aquatic environment and fish in a large antimony mining area in Hunan, China. Sci. Total Environ. 408, 3403–3410.
Fu, Z., Wu, F., Mo, C., Deng, Q., Meng, W., Giesy, J.P., 2016. Comparison of arsenic and antimony biogeochemical behavior in water, soil and tailings from Xikuangshan, China. Sci. Total Environ. 539, 97–104.
Furuta, N., Iijima, A., Kambe, A., Sakai, K., Sato, K., 2005. Concentrations, enrichment and predominant sources of Sb and other trace elements in size classified airborne particulate matter collected in Tokyo from 1995 to 2004. J. Environ. Monit. 7, 1155–1161.
Gebel, T., Christensen, S., Dunkelberg, H., 1997. Comparative and environmental genotoxicity of antimony and arsenic. Anticancer Res. 17, 2603–2607.
Grafe, M., Eick, M., Grossl, P., 2001. Adsorption of arsenate (V) and arsenite (III) on goethite in the presence and absence of dissolved organic carbon. Soil Sci. Soc. Am. J. 65, 1680–1687.
Guo, X., Wu, Z., He, M., 2009. Removal of antimony (V) and antimony (III) from drinking water by coagulation–flocculation–sedimentation (CFS). Water Res. 43, 4327–4335.
Guo, X., Wu, Z., He, M., Meng, X., Jin, X., Qiu, N., Zhang, J., 2014. Adsorption of antimony onto iron oxyhydroxides: adsorption behavior and surface structure. J. Hazard. Mater. 276, 339–345.
Guo, J., Su, L., Zhao, X., Xu, Z., Chen, G., 2016. Relationships between urinary antimony levels and both mortalities and prevalence of cancers and heart diseases in general US population, NHANES 1999–2010. Sci. Total Environ. 571, 452–460.
He, M., Wang, X., Wu, F., Fu, Z., 2012. Antimony pollution in China. Sci. Total Environ. 421–422, 41–50.
Herath, I., Vithanage, M., Bundschuh, J., 2017. Antimony as a global dilemma: geochemistry, mobility, fate and transport. Environ. Pollut. 223, 545–559.
Hering, J.G., Chen, P.-Y., Wilkie, J.A., Elimelech, M., 1997. Arsenic removal from drinking water during coagulation. J. Environ. Eng. 123, 800–807.
Jiang, J., Graham, N., 1998. Observations of the comparative hydrolysis/precipitation behaviour of polyferric sulphate and ferric sulphate. Water Res. 32, 930–935.
Jiang, J.-Q., Graham, N.J.D., Harward, C., 1993. Comparison of polyferric sulphate with other coagulants for the removal of algae and algae-derived organic matter. Water Sci. Technol. 27, 221–230.
Johnson, C.A., Moench, H., Wersin, P., Kugler, P., Wenger, C., 2005. Solubility of antimony and other elements in samples taken from shooting ranges. J. Environ. Qual. 34, 248–254.
Kang, M., Kawasaki, M., Tamada, S., Kamei, T., Magara, Y., 2000. Effect of pH on the removal of arsenic and antimony using reverse osmosis membranes. Desalination 131, 293–298.
Kang, M., Kamei, T., Magara, Y., 2003. Comparing polyaluminum chloride and ferric chloride for antimony removal. Water Res. 37, 4171–4179.
Kong, L., He, M., Hu, X., 2016. Rapid photooxidation of Sb (III) in the presence of different Fe (III) species. Geochim. Cosmochim. Acta 180, 214–226.
Kurniawan, T.A., Chan, G.Y., Lo, W.-H., Babel, S., 2006. Physico–chemical treatment techniques for wastewater laden with heavy metals. Chem. Eng. J. 118, 83–98.
Liu, F., Le, X.C., McKnight-Whitford, A., Xia, Y., Wu, F., Elswick, E., Johnson, C.C., Zhu, C., 2010. Antimony speciation and contamination of waters in the Xikuangshan antimony mining and smelting area, China. Environ. Geochem. Health 32, 401–413.
Luo, J., Luo, X., Crittenden, J., Qu, J., Bai, Y., Peng, Y., Li, J., 2015. Removal of antimonite (Sb (III)) and antimonate (Sb (V)) from aqueous solution using carbon nanofibers that are decorated with zirconium oxide (ZrO_2). Environ. Sci. Technol. 49, 11115–11124.
Matijević, E., Scheiner, P., 1978. Ferric hydrous oxide sols. J. Colloid Interface Sci. 63, 509–524.
Mitsunobu, S., Takahashi, Y., Terada, Y., Sakata, M., 2010. Antimony (V) incorporation into synthetic ferrihydrite, goethite, and natural iron oxyhydroxides. Environ. Sci. Technol. 44, 3712–3718.

Mitsunobu, S., Muramatsu, C., Watanabe, K., Sakata, M., 2013. Behavior of antimony (V) during the transformation of ferrihydrite and its environmental implications. Environ. Sci. Technol. 47, 9660–9667.
Okkenhaug, G., Zhu, Y.-G., Luo, L., Lei, M., Li, X., Mulder, J., 2011. Distribution, speciation and availability of antimony (Sb) in soils and terrestrial plants from an active Sb mining area. Environ. Pollut. 159, 2427–2434.
Okkenhaug, G., Zhu, Y.-G., He, J., Li, X., Luo, L., Mulder, J., 2012. Antimony (Sb) and arsenic (As) in Sb mining impacted paddy soil from Xikuangshan, China: differences in mechanisms controlling soil sequestration and uptake in rice. Environ. Sci. Technol. 46, 3155–3162.
Poon, R., Chu, I., Lecavalier, P., Valli, V., Foster, W., Gupta, S., Thomas, B., 1998. Effects of antimony on rats following 90-day exposure via drinking water. Food Chem. Toxicol. 36, 21–35.
SAC (Standardization Administration of the People's Republic of China), 2002. Standards for Surface Water Quality, GB-3838-2002.
Schnorr, T.M., Steenland, K., Thun, M.J., Rinsky, R.A., 1995. Mortality in a cohort of antimony smelter workers. Am. J. Ind. Med. 27, 759–770.
Shan, C., Ma, Z., Tong, M., 2014. Efficient removal of trace antimony (III) through adsorption by hematite modified magnetic nanoparticles. J. Hazard. Mater. 268, 229–236.
Steely, S., Amarasiriwardena, D., Xing, B., 2007. An investigation of inorganic antimony species and antimony associated with soil humic acid molar mass fractions in contaminated soils. Environ. Pollut. 148, 590–598.
Ungureanu, G., Santos, S., Boaventura, R., Botelho, C., 2015. Arsenic and antimony in water and wastewater: overview of removal techniques with special reference to latest advances in adsorption. J. Environ. Manag. 151, 326–342.
USEPA, 1979. Water Related Fate of the 129 Priority Pollutants. vol. 1. USEPA, Washington, DC, USA.
Wang, X., He, M., Xi, J., Lu, X., 2011. Antimony distribution and mobility in rivers around the world's largest antimony mine of Xikuangshan, Hunan Province, China. Microchem. J. 97, 4–11.
WHO, 2004. Guidelines for Drinking-water Quality. World Health Organization, Geneva.
Wu, Z., He, M., Guo, X., Zhou, R., 2010. Removal of antimony (III) and antimony (V) from drinking water by ferric chloride coagulation: competing ion effect and the mechanism analysis. Sep. Purif. Technol. 76, 184–190.
Wu, F., Fu, Z., Liu, B., Mo, C., Chen, B., Corns, W., Liao, H., 2011. Health risk associated with dietary co-exposure to high levels of antimony and arsenic in the world's largest antimony mine area. Sci. Total Environ. 409, 3344–3351.
Wu, F., Sun, F., Wu, S., Yan, Y., Xing, B., 2012. Removal of antimony (III) from aqueous solution by freshwater cyanobacteria *Microcystis* biomass. Chem. Eng. J. 183, 172–179.
Xi, J., He, M., Wang, K., Zhang, G., 2013. Adsorption of antimony (III) on goethite in the presence of competitive anions. J. Geochem. Explor. 132, 201–208.
Zhang, X., 2016. Antimony pollution accident of Gansu Longxing enterprise and emergent water supply in Guangyuan City. Water Waste Eng. 42, 9–20 (in Chinese).
Zhao, X., Dou, X., Mohan, D., Pittman, C.U., Ok, Y.S., Jin, X., 2014. Antimonate and antimonite adsorption by a polyvinyl alcohol-stabilized granular adsorbent containing nanoscale zero-valent iron. Chem. Eng. J. 247, 250–257.
Zhu, J., Wu, F., Deng, Q., Shao, S., Mo, C., Pan, X., Li, W., Zhang, R., 2009. Environmental characteristics of water near the Xikuangshan antimony mine, Hunan Province. Acta Sci. Circumst. 29, 655–661.
Zhu, J., Wu, F., Pan, X., Guo, J., Wen, D., 2011. Removal of antimony from antimony mine flotation wastewater by electrocoagulation with aluminum electrodes. J. Environ. Sci. 23, 1066–1071.
Zou, J.-P., Liu, H.-L., Luo, J., Xing, Q.-J., Du, H.-M., Jiang, X.-H., Luo, X.-B., Luo, S.-L., Suib, S.L., 2016. Three-dimensional reduced graphene oxide coupled with Mn_3O_4 for highly efficient removal of Sb (III) and Sb (V) from water. ACS Appl. Mater. Interfaces 8, 18140–18149.

Removal of antimonate (Sb(V)) and antimonite (Sb(III)) from aqueous solutions by coagulation-flocculation-sedimentation (CFS): Dependence on influencing factors and insights into removal mechanisms

WenjingGuo [a, b],Zhiyou Fu [b*], Hao Wang [a, b], Shasha Liu [b], Fengchang Wu [b], John P. Giesy [b c]

[a] *College of Water Sciences, Beijing Normal University, Beijing 100875, China*

[b] *State Key Laboratory of Environment Criteria and Risk Assessment, Chinese Research Academy of Environmental Sciences, Beijing 100012, China*

[c]*Department of Biomedical and Veterinary Biosciences and Toxicology Centre, University of Saskatchewan, Saskatoon, Saskatchewan, Canada*

* *Corresponding author: Zhiyou Fu, zhiyoufu@126.com. +86-10-84915312*

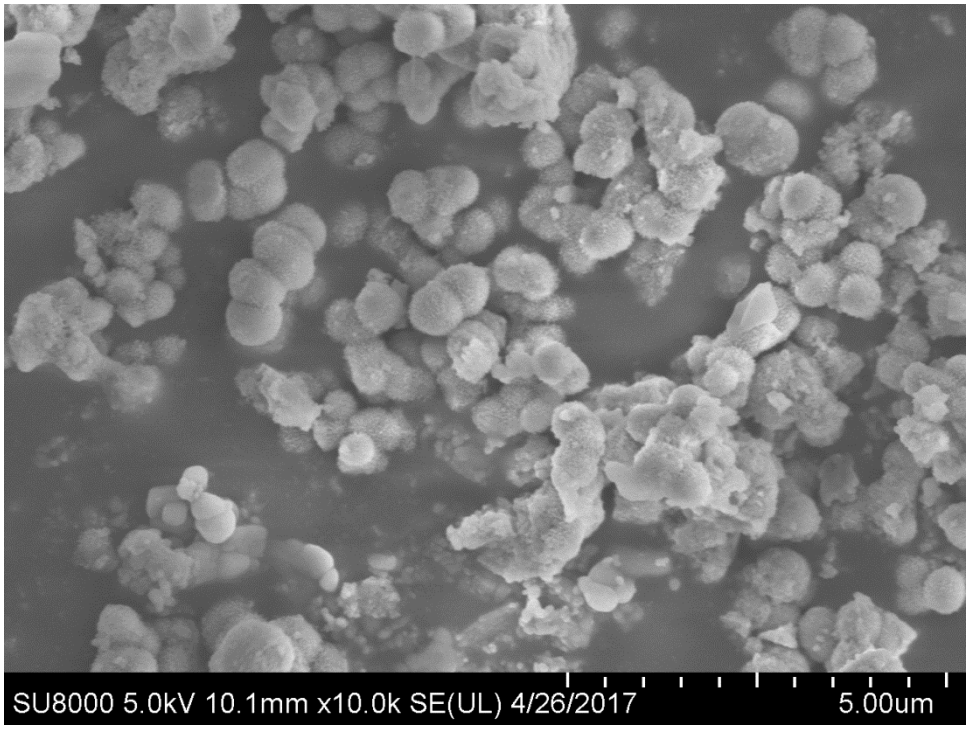

Fig. S1 SEM images of pure hydrolysate of PFS (pH: 5.0 ± 1.0).

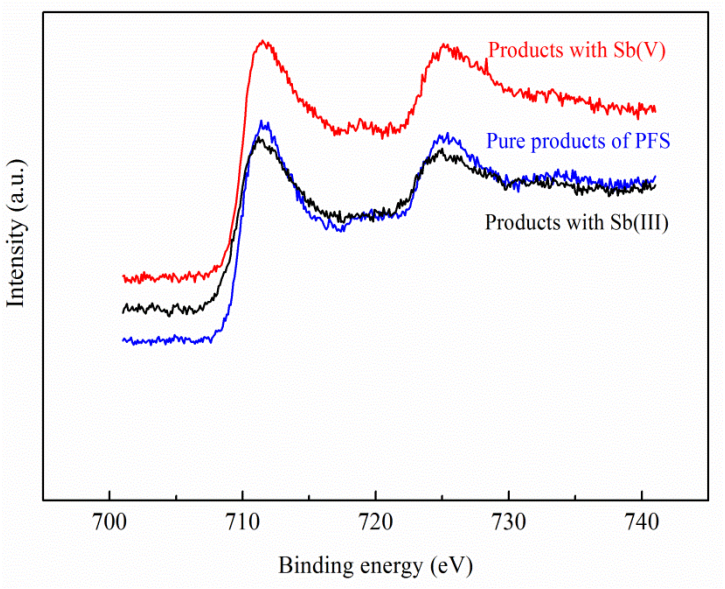

Fig. S2 X-ray photoelectron spectroscopy (XPS) characterization of Fe 2p of pure polymeric ferric sulfate (PFS), PFS bound to Sb(V) and PFS bound to Sb(III).

Table S1 Details of X-ray photoelectron spectroscopy (XPS) fitting results.

Sample	Ratio	Binding energy (eV)				
	O_{ad}/Sb $3d_{5/2}$	O_{latt}	O_{ad}	O_{H2O}	Sb $3d_{3/2}$	Sb $3d_{5/2}$
Pure polymeric ferric sulfate (PFS)	/	530.19	531.72	533.29	/	/
PFS loading with Sb(V)	0.48	/	532.06	534.02	530.62	540.19
PFS loading with Sb(III)	0.77	/	531.74	533.26	530.29	539.77

Table S2 The physical and chemical parameters in typical contaminated waters from the Xikuangshan mining area.

Sample types	Sb(V) (μg/L)	Sb(III) (μg/L)	Electric conductivity (ms/m)	DO (mg/L)	Fe (μg/L)	Zn (μg/L)	Se (μg/L)
River water	19.0	N.D.	41	5.5	N.D.	4.3	11.0
Retained water	7.6	N.D.	64.1	11.1	43.1	1175.4	N.D.
Well water	10.7	N.D.	43.2	2.2	174.8	1625.0	N.D.

N.D. represented not detected.

Table S3 Removal performances by using PFS via CFS process in typical contaminated waters.

Sample types	Residual concentration of waters with stock solutions (μg/L)		Removal percentage (%)	
	Sb(V)	Sb(III)	Sb(V)	Sb(III)
River water	10.0	1.7	96.0	98.3
Retained water	5.5	1.3	97.9	98.7
Well water	6.3	1.9	97.6	98.1